Machine Learning Based Selective Electrochemical Analysis of Dopamine, Uric Acid, and Ascorbic Acid

Muhsin Mert Tekin, Ece Minel Bursalı, Mustafa Şen, Volkan Kılıç
Department of Biomedical Engineering
Department of Electrical Electronical Engineering
Izmir Katip Celebi University, Izmir, Turkey
muhsinmerttekin@gmail.com, eceminelbursali@gmail.com,
mustafa.sen@ikcu.edu.tr, volkan.kilic@ikcu.edu.tr

***Abstract*—This study presents a machine learning-based approach for the simultaneous and selective electrochemical analysis of dopamine (DA), uric acid (UA), and ascorbic acid (AA). These biomolecules often coexist in biological samples. Traditional methods struggle with resolution and precision, particularly in the presence of mixed solutions. To overcome these challenges, a system was developed in which artificial intelligence (AI) was trained using electrochemical data from mixtures of varying concentrations of DA, UA, and AA. The AI model was designed to identify patterns in the electrochemical signals and plot the deconvoluted graphs. Differential Pulse Voltammetry (DPV) was employed as the electrochemical technique, with screen-printed electrodes (SPEs) used to measure the redox behavior of each acid. The resulting data underwent baseline correction, peak deconvolution, and feature extraction to generate a dataset for training machine learning classifiers. By analyzing the experimental data alongside deconvoluted peak features, the model achieved enhanced accuracy in plotting the desired graphs. The integration of this AI model into a MATLAB-based application provides a user-friendly interface that promises significant advances in electrochemical sensor technology for biomedical applications. This work demonstrates the potential of machine learning to improve the selectivity and precision of electrochemical analysis, offering a powerful tool for multi-analyte detection in clinical and research settings.**

Keywords*—*Electrochemical Analysis, Machine Learning (ML), Artificial Intelligence (AI), Differential Pulse Voltammetry (DPV), Screen-Printed Electrodes (SPEs).

I. Introduction

The simultaneous and selective detection of biomolecules such as dopamine (DA), uric acid (UA), and ascorbic acid (AA) is crucial in clinical diagnostics and biomedical research. These molecules often coexist in biological samples, leading to complex electrochemical signals. While traditional methods provide useful insights, they struggle with accuracy and precision, particularly in complex mixtures. [1] [2]

This project addresses these challenges by applying machine learning techniques to enhance the selectivity and accuracy of electrochemical analysis. Specifically, a system was proposed in which AI learns from electrochemical data obtained from mixtures of DA, UA, and AA at various concentrations. By analyzing the resulting data patterns, the AI model was trained to plot the deconvoluted graphs from the combined graph. [3]

The approach focuses on using AI to process the data from electrochemical signals, which reflect the oxidation and reduction behaviors of the acids. By learning the relationships between the data patterns and the corresponding concentrations, the AI model developed the capability to accurately predict the concentration of each molecule in future experiments. Additionally, an application was developed using MATLAB's App Designer to integrate the AI model, providing a user-friendly interface for real-time analysis and prediction.

This project aims to advance electrochemical sensor technology for biomedical applications, offering an innovative approach to multi-analyte detection through the integration of machine learning. By learning from electrochemical data, the AI system promises enhanced accuracy and efficiency in detecting these important biomolecules.

II. Method

A. Dopamine

DPV was used as an electrochemical technique to measure the concentration of DA in solution. In this method, a series of voltage pulses applied along a gradually increasing voltage sweep were introduced to an electrochemical cell. The current was measured just before and at the end of each pulse, and the difference between these values was recorded as the response. SPEs, consisting of a working electrode, a reference electrode, and a counter electrode, were employed in the setup. DA underwent redox reactions at the working electrode, while the reference electrode maintained a constant potential, and the counter electrode facilitated current flow.

Phosphate-buffered saline (PBS) was prepared by dissolving one tablet in 200 mL of deionized water and was used to dilute the DA stock solution. DA concentrations were selected based on previous studies involving SPEs and were prepared using calculated volumes of PBS. [4] The prepared solutions were subjected to DPV measurements to analyze their electrochemical behavior.

978-1-6654-3649-6/21/$31.00 ©2021 IEEE

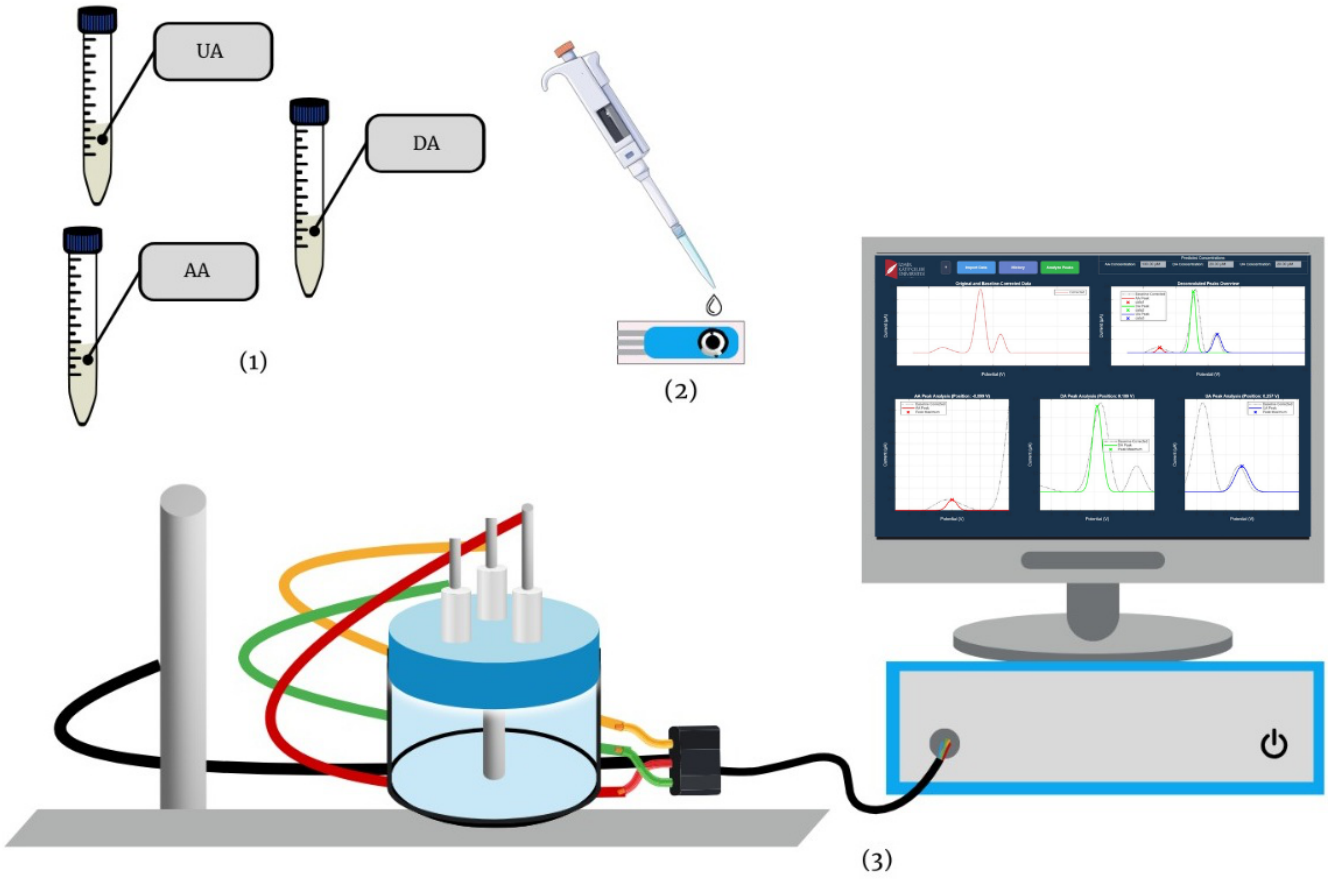

Figure 1: Schematic representation of (1) used molecules, (2) dropping solutions onto the electrode surface, (3) making DPV measurements by connecting the system to a computer.

B. Uric Acid

The analysis of UA was conducted using DPV with SPEs in a similar setup. A 1 mM stock solution of UA was prepared by accurately weighing and dissolving the required amount in PBS. This stock solution was then diluted to achieve final concentrations of 500, 250, 100, 50, 20, 10, and 5 µM.

Each solution was dropped onto SPE, and the DPV measurements were recorded to determine the electrochemical responses of UA. Between measurements, the electrode was cleaned thoroughly with deionized water (DIW) to prevent contamination, ensuring accurate readings.

C. Ascorbic Acid

The DPV analysis of AA followed the same method as for DA and UA. A 1 mM stock solution was prepared using PBS, which was then diluted to obtain concentrations comparable to those of the other analytes.

Since the experiments conducted with AA initially did not yield the expected results, the same experiments were repeated using multi-walled carbon nanotube (MWCNT)-modified electrodes. After repeating the experiments with MWCNT-modified electrodes, better results were better obtained.

The prepared solutions were analyzed using the SPE setup under the same conditions, with care taken to clean the electrodes between tests. A Faraday cage was used during the measurements to minimize noise and improve the accuracy of the results.

D. Combined Analysis

Experiments involving the combination of DA, UA, and AA were performed to study their interactions and individual contributions within mixed solutions as shown in the Figure 1. A total of 27 mixtures were prepared by choosing concentrations of 20, 50, and 100 µM for each of the three acids. These concentrations were selected to explore a range of possible interactions. Initial calculations were carried out to determine the appropriate volumes of each acid to achieve the desired concentrations in the mixtures. A table summarizing these values was prepared to ensure accurate preparation.

The solutions were prepared by mixing the acids in the calculated proportions, and DPV measurements were conducted to analyze their combined electrochemical behavior.

To minimize variability, all measurements were conducted under identical experimental conditions, ensuring consistency across trials. The collected data were systematically analyzed to identify patterns and assess the influence of different concentration combinations. [5] [6] The final results were exported to Excel for creating and visualizing the data in detailed graphs. Machine learning models created to integrate them in the application.

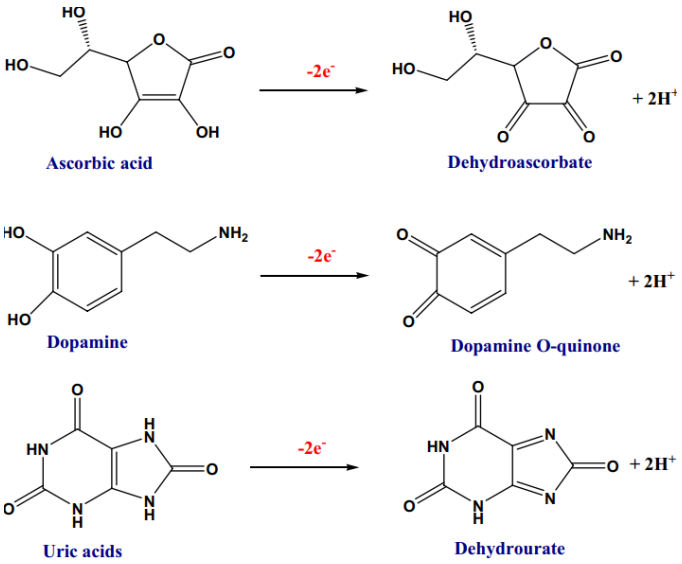

Figure 2: Schematic illustration for the electro-oxidation mechanism of AA, DA and UA. [7]

E. Dataset Preparation for Machine Learning

The preparation of the dataset began with baseline correction performed on each combined graph individually. This step ensured that any unwanted offsets in the data were eliminated, allowing for more accurate analysis. Following baseline correction, a peak deconvolution algorithm was applied as shown in the Figure 3. This algorithm enabled the separation of the combined graph, which contained three peaks, into three distinct graphs corresponding to DA, UA, and AA. [8]

From the deconvoluted graphs, critical features were extracted for each acid, including the x-coordinates and y-coordinates of the peaks, as well as the variance. These extracted features were then used to create the output columns in the dataset, which were utilized in training machine learning classifiers. The features were carefully selected based on the distinct characteristics of the peaks in the electrochemical graphs. Each acid in the mixture exhibits unique peak features that can be modeled with a Gaussian function. These peak-related features serve as effective indicators for the concentration of each acid in the mixture. The x-coordinate corresponds to the peak position, the y-coordinate represents the peak intensity, and the variance captures the spread or width of the peak. These features were chosen for their ability to represent the unique characteristics of Gaussian-like peaks produced by electrochemical data. [9]

Next, the data was categorized by determining the highest and lowest points for each feature, and the range was divided into six categories. In total, nine classifiers were developed for these three features.

When creating the input features, a different approach was taken compared to the output labels. Instead of performing peak deconvolution, the combined graphs were used directly. This was done to provide the model with the actual electrochemical signal data, which includes the interaction between the different acids in the mixture. These combined graphs reflect the complex relationships between the acids in a real experimental setting.

For the output labels, the peak deconvoluted versions of the graphs were used. Deconvolution allowed for the separation of the peaks of the three acids into distinct, individual components, which facilitated the identification of each acid's contribution to the combined signal. In essence, the model was trained to predict the peak deconvoluted data (i.e., the separate peaks of each acid) based on the combined graph input. This setup enabled the model to draw the predicted graphs for each acid. Additionally, three more classifiers were prepared, with the output column labeled according to the concentration of each acid. This helped the model learn to differentiate and predict the concentration of each acid in a mixed solution.

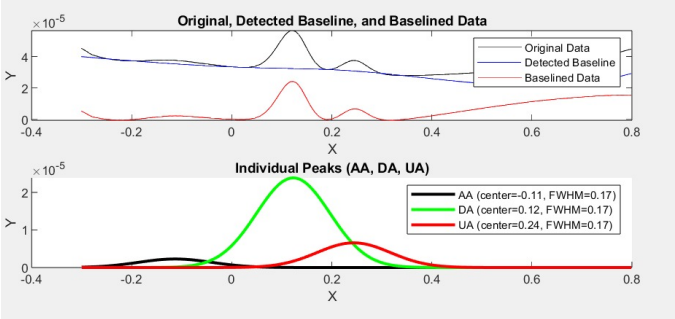

Figure 3: Image showing the actual values calculated using the MATLAB code for peak deconvolution analysis. These values represent the true values derived from the dataset for the AA, DA, and UA respectively.

Once the classifiers were prepared, to optimize the performance of the classifiers, a code was developed that systematically tested different random seed numbers, selecting the best-performing seed after evaluating the results of 100 different seed values. The use of random seeds is essential for ensuring the model's robustness and generalizability, as it helps avoid overfitting to any specific data split. [10]

The selected seed number and model, which yielded the best results in terms of training accuracy and prediction performance, were then used to train the models for each of the twelve classifiers and were integrated into the desktop application as shown in the Figure 5. This process ensured that the models were optimized and capable of providing reliable predictions when applied to new, unseen data.

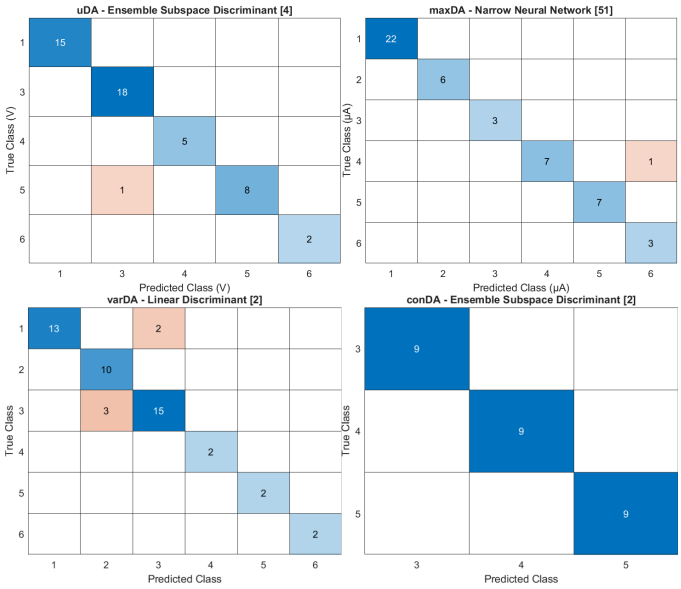

Figure 4: Confusion matrix tables of the features of DA with the best-performing models and seed numbers.

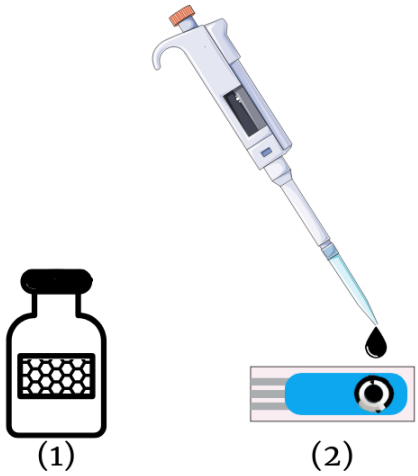

Figure 5: Schematic illustration of (1) MWCNT solution, (2) modification process of SPE.

F. The Proposed Approach

The proposed approach aims to address the challenges of simultaneous and selective detection of DA, UA, and AA in complex mixtures by integrating DPV with machine learning techniques. DPV was chosen as the electrochemical method due to its sensitivity and ability to generate distinct oxidation and reduction peaks for the target biomolecules. To enhance signal clarity and resolution, MWCNT-modified electrodes were employed, providing improved conductivity and peak separation compared to unmodified electrodes.

For data analysis, a machine learning model was developed to process the electrochemical signals directly from the combined graphs without requiring peak deconvolution. This approach leverages the experimental data to capture the unique interactions between the biomolecules in the mixture. The model was trained on DPV measurements from single-analyte solutions and mixed solutions, covering a range of concentrations to ensure robust performance.

The experimental evaluations were conducted to assess the effectiveness of the proposed approach in detecting and quantifying DA, UA, and AA in both individual and mixed solutions. The experiments aimed to validate the electrochemical setup, optimize electrode modifications, and evaluate the performance of the machine learning model.

DPV was utilized to characterize the oxidation and reduction behaviors of the three analytes. Initial experiments were performed using unmodified SPEs, which provided basic insights into the electrochemical responses of DA, UA, and AA. However, AA exhibited poorly resolved peaks, necessitating further optimization.

To address the low resolution of AA peaks, MWCNT-modified electrodes were employed as shown in the Figure 4. The modified electrodes significantly enhanced the peak intensity and resolution for all three analytes. This improvement was particularly notable for AA, whose peaks became distinct and well-defined after modification.

Mixtures of DA, UA, and AA were prepared at concentrations of 20, 50, and 100 μM to evaluate the system's ability to detect and quantify individual components in complex solutions. DPV measurements of these mixtures demonstrated well-separated peaks for each analyte, confirming the effectiveness of the optimized setup.

Machine learning models were used to analyze the combined DPV signals directly. The model was trained using a dataset comprising DPV measurements from individual solutions and mixtures. The training dataset included critical features such as peak intensity, position, and variance. The model's performance was evaluated using test data. Key metrics such as accuracy, precision, recall, and F1-score were calculated to assess the model's performance, as shown in Table 1. Additionally, MAE, MSE, and RMSE were calculated, as shown in Table 2. [11]

G. Dataset and Performance Metrics

$$\text{Accuracy} = \frac{TP + TN}{TP + TN + FP + FN} \tag{1}$$

$$\text{Precision} = \frac{TP}{TP + FP} \tag{2}$$

$$\text{Recall} = \frac{TP}{TP + FN} \tag{3}$$

$$F1 = 2 \times \frac{\text{Precision} \times \text{Recall}}{\text{Precision} + \text{Recall}} \tag{4}$$

Molecule	Feature	Seed Number & Model Type & Preset	Accuracy	Precision	Recall	F1 Score
Ascorbic Acid (AA)	uAA	[80] Ensemble Bagged Trees	0.89	0.83	0.89	0.82
	maxAA	[72] Fine Tree	0.67	0.58	0.58	0.67
	varAA	[32] Weighted KNN	0.67	0.67	0.70	0.79
	conAA	[20] Ensemble Subspace KNN	0.77	0.79	0.77	0.78
Dopamine (DA)	uDA	[4] Ensemble Subspace Discriminant	0.78	0.67	0.78	0.87
	maxDA	[51] Narrow Neural Network	0.89	0.92	0.80	0.95
	varDA	[2] Linear Discriminant	0.78	0.56	0.50	0.90
	conDA	[2] Ensemble Subspace Discriminant	0.89	0.90	0.89	0.88
Uric Acid (UA)	uUA	[6] Linear SVM	0.89	0.79	0.89	0.92
	maxUA	[23] Fine Tree	0.78	0.60	0.83	0.89
	varUA	[6] Fine KNN	0.78	0.75	0.87	0.91
	conUA	[13] Ensemble RUS Boosted Trees	0.66	0.58	0.62	0.62

Table I: Performance metrics of electrochemical analysis of AA, DA and UA.

Molecule	Feature	Classifier Model Type	Preset	Seed Number	MAE	MSE	RMSE
Ascorbic Acid (AA)	uAA	Ensemble	Bagged Trees	80	0.04743975	0.00225053	0.04743975
	maxAA	Tree	Fine Tree	72	0.00000077	0.00000077	0.00000077
	varAA	KNN	Weighted KNN	37	0.15649637	0.02449137	0.15649718
Dopamine (DA)	uDA	Ensemble	Subspace Discriminant	4	0.00665685	0.00004432	0.00665709
	maxDA	Neural Network	Narrow Neural Network	51	0.00000221	0.00000222	0.00000222
	varDA	Discriminant	Linear Discriminant	2	0.15576747	0.02426356	0.15576764
Uric Acid (UA)	uUA	SVM	Linear SVM	6	0.06814000	0.00464306	0.06814000
	maxUA	Tree	Fine Tree	23	0.00000161	0.00000161	0.00000161
	varUA	KNN	Fine KNN	6	0.14860535	0.02208370	0.14860587

Table II: Performance of classifier models for predicting features of AA, DA and UA.

H. Results and Discussion

DPV was employed to study the electrochemical behavior of DA, UA, and AA, both individually and in mixed solutions. For the individual solutions, distinct peaks were observed for each biomolecule, corresponding to their unique redox potentials. DA, UA, and AA produced well-defined electrochemical signals, confirming the sensitivity and selectivity of the experimental setup using SPEs and PBS.

In the case of AA, the initial experiments exhibited lower signal quality. This issue was addressed by employing MWCNT-modified electrodes, which significantly improved the resolution and intensity of the AA signal. The modified electrodes effectively enhanced the electron transfer kinetics, ensuring reliable detection of AA in both individual and mixed solutions.

The dataset for machine learning training was constructed by extracting the features from the deconvoluted graphs. The machine learning model was trained on the combined graphs, bypassing the deconvolution process for input features, allowing it to directly interpret experimental data.

The classifiers achieved high accuracy in predicting the concentrations of DA, UA, and AA from the combined signals. Systematic testing of random seed values during training ensured robust and generalized model performance. The optimized seed resulted in minimal prediction errors and consistent accuracy across all twelve classifiers. This highlights the importance of random seed selection in enhancing model reliability. [12] This study underscores the potential of integrating machine learning into electrochemical analysis for biomedical applications. The developed system provides a scalable and efficient approach for multi-analyte detection, which could be extended to other biomolecules or clinical scenarios. Future work could explore the incorporation of additional features, or advanced signal processing techniques, to further enhance model performance. Additionally, expanding the dataset to include broader concentration ranges and real biological samples could improve the generalizability and clinical relevance of the system.

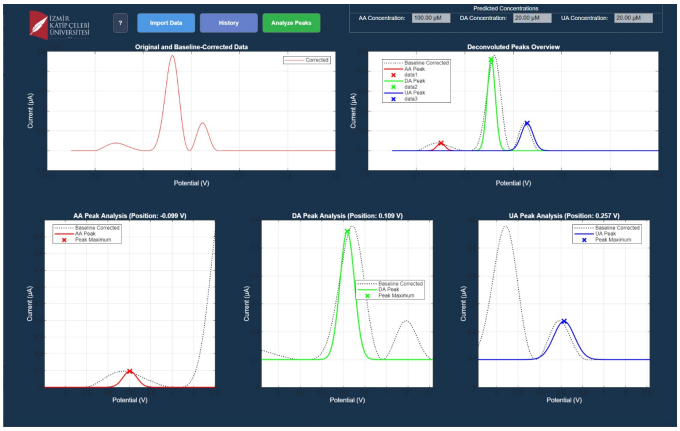

Figure 6: Image showing the predicted graphs generated by the machine learning algorithm, representing the peak deconvolution results for AA, DA, and UA respectively using trained classifier models integrated in the application.

III. Future Directions and Challenges

Future research in machine learning-based electrochemical analysis of DA, UA, and AA faces several key challenges while offering promising opportunities. One significant challenge lies in converting laboratory results to real-world biological samples, where additional interfering compounds and matrix

effects could complicate detection. The development of more robust electrode modifications and advanced data preprocessing techniques will be crucial to address these issues. There is also potential to expand the system's capabilities by incorporating real-time analysis features and developing portable, smartphone-integrated devices for point-of-care diagnostics. The machine learning model could be enhanced by incorporating deep learning architectures and expanding the training dataset to include a wider range of concentrations. Additionally, investigating the system's performance with other biomolecules of clinical interest could broaden its applications in medical diagnostics.

Integration with emerging technologies such as Internet of Things (IoT) platforms could enable remote monitoring and data collection, though this would require addressing challenges related to data security and standardization. Another promising direction involves developing adaptive calibration methods to account for electrode degradation over time. The ultimate goal would be to create a versatile, reliable platform that can be deployed in clinical settings while maintaining high accuracy and reproducibility across different conditions.

IV. Conclusion

This study successfully demonstrated the simultaneous and selective detection of DA, UA, and AA in mixtures using DPV coupled with machine learning techniques. By optimizing experimental conditions, including the utilization of MWCNT-modified electrodes, the electrochemical signals of each biomolecule were effectively resolved. The integration of artificial intelligence further strengthened the analytical capabilities by enabling concentration predictions based on distinct electrochemical response patterns.

The combination of DPV and machine learning represents a significant advancement in electrochemical sensing, offering a rapid and cost-effective approach to multi-analyte detection. The findings underscore the potential of AI-driven electrochemical analysis in clinical diagnostics, particularly for detecting and monitoring biomolecules.

Furthermore, this approach could be extended to a broader range of biomolecules and disease markers, facilitating early disease diagnosis and personalized medicine. Future research could focus on refining the machine learning algorithms to handle a larger dataset, improving model generalization for real-world applications. Additionally, advancements in electrode surface modifications, including the development of nanomaterial-based sensors, could further enhance sensitivity and selectivity. The implementation of real-time analysis systems and portable electrochemical sensors would pave the way for point-of-care diagnostics, environmental monitoring, and biomedical research.

In conclusion, this study lays the groundwork for a more efficient approach to electrochemical sensing. By harnessing the power of AI, the proposed methodology offers new possibilities for improving diagnostic accuracy and expanding the capabilities of electrochemical analysis in various scientific and medical fields. Continued research in this area will contribute to the development of next-generation biosensors with enhanced performance, real-time capabilities, and widespread applicability.

References

[1] D. Ji, Z. Liu, L. Liu, S. S. Low, Y. Lu, X. Yu, L. Zhu, C. Li, and Q. Liu, "Smartphone-based integrated voltammetry system for simultaneous detection of ascorbic acid, dopamine, and uric acid with graphene and gold nanoparticles modified screen-printed electrodes," *Biosensors and Bioelectronics*, vol. 119, pp. 55–62, 2018. [Online]. Available: https://www.sciencedirect.com/science/article/pii/S0956566318305840

[2] N. Tukimin, J. Abdullah, and Y. Sulaiman, "Review—electrochemical detection of uric acid, dopamine and ascorbic acid," *Journal of The Electrochemical Society*, vol. 165, no. 7, p. B258, apr 2018. [Online]. Available: https://dx.doi.org/10.1149/2.0201807jes

[3] V. Kammarchedu, D. Butler, and A. Ebrahimi, "A machine learning-based multimodal electrochemical analytical device based on emosx-lig for multiplexed detection of tyrosine and uric acid in sweat and saliva," *Analytica Chimica Acta*, vol. 1232, p. 340447, Nov 2022, epub 2022 Sep 29. [Online]. Available: https://doi.org/10.1016/j.aca.2022.340447

[4] B. Habibi, M. Jahanbakhshi, and M. H. Pournaghi-Azar, "Simultaneous determination of acetaminophen and dopamine using swcnt modified carbon–ceramic electrode by differential pulse voltammetry," *Electrochimica Acta*, vol. 56, no. 7, pp. 2888–2894, 2011. [Online]. Available: https://www.sciencedirect.com/science/article/pii/S0013468610017354

[5] K. Kunpatee, S. Traipop, O. Chailapakul, and S. Chuanuwatanakul, "Simultaneous determination of ascorbic acid, dopamine, and uric acid using graphene quantum dots/ionic liquid modified screen-printed carbon electrode," *Sensors and Actuators B: Chemical*, vol. 314, p. 128059, 2020. [Online]. Available: https://www.sciencedirect.com/science/article/pii/S0925400520304093

[6] J. Ping, J. Wu, Y. Wang, and Y. Ying, "Simultaneous determination of ascorbic acid, dopamine and uric acid using high-performance screen-printed graphene electrode," *Biosensors and Bioelectronics*, vol. 34, no. 1, pp. 70–76, 2012. [Online]. Available: https://www.sciencedirect.com/science/article/pii/S0956566312000346

[7] P. Sakthivel, K. Ramachandran, K. Maheshvaran, T. S. Senthil, and P. Manivel, "Simultaneous electrochemical detection of ascorbic acid, dopamine and uric acid using au decorated carbon nanofibers modified screen printed electrode," *Carbon Letters*, vol. 34, no. 9, pp. 2325–2341, 2024.

[8] N. Schmid, S. Bruderer, F. Paruzzo, G. Fischetti, G. Toscano, D. Graf, M. Fey, A. Henrici, V. Ziebart, B. Heitmann, H. Grabner, J. Wegner, R. Sigel, and D. Wilhelm, "Deconvolution of 1d nmr spectra: A deep learning-based approach," *Journal of Magnetic Resonance*, vol. 347, p. 107357, 2023. [Online]. Available: https://www.sciencedirect.com/science/article/pii/S1090780722002154

[9] J. Liu and F. Ciucci, "The gaussian process distribution of relaxation times: A machine learning tool for the analysis and prediction of electrochemical impedance spectroscopy data," *Electrochimica Acta*, vol. 331, p. 135316, 2020. [Online]. Available: https://www.sciencedirect.com/science/article/pii/S0013468619321887

[10] S. Dutta, A. Arunachalam, and S. Misailovic, "To seed or not to seed? an empirical analysis of usage of seeds for testing in machine learning projects," in *2022 IEEE Conference on Software Testing, Verification and Validation (ICST)*, 2022, pp. 151–161.

[11] T. Shaikhina, D. Lowe, S. Daga, D. Briggs, R. Higgins, and N. Khovanova, "Machine learning for predictive modelling based on small data in biomedical engineering," *IFAC-PapersOnLine*, vol. 48, no. 20, pp. 469–474, 2015, 9th IFAC Symposium on Biological and Medical Systems BMS 2015. [Online]. Available: https://www.sciencedirect.com/science/article/pii/S2405896315020765

[12] S. N. A. B. M. Nashruddin, F. H. M. Salleh, R. M. Yunus, and H. B. Zaman, "Artificial intelligencepowered electrochemical sensor: Recent advances, challenges, and prospects," *Heliyon*, vol. 10, no. 18, p. e37964, 2024. [Online]. Available: https://www.sciencedirect.com/science/article/pii/S2405844024139953